ELECTRIC FIELD AND PLASMA OBSERVATIONS IN THE MAGNETOSPHERE

Donald A. Gurnett
Department of Physics and Astronomy, The University of Iowa
Iowa City, Iowa   52240   U.S.A.

Abstract. Satellite-borne electric field measurements using the double-
probe technique have now provided a comprehensive survey of convection
electric fields at low altitudes in the magnetosphere. The most prominent
features of the convection electric fields are reversals located at
high magnetic latitudes, with generally anti-sunward convection poleward
and sunward convection equatorward of the electric field reversal loca-
tion. The electric field reversal is usually coincident with the "trapping
boundary" for electrons with energies $E > 45$ keV and is interpreted as the
boundary between open and closed magnetic field lines. On the day side of
the magnetosphere the electric field reversal is observed to coincide with
the equatorward boundary of the polar cusp. In the local afternoon and
evening regions "inverted V" electron precipitation bands occur at or near
the electric field reversal and in regions usually characterized by large
fluctuations in the electric field. In the local midnight region strong
convection electric fields have also been observed deep within the magneto-
sphere, near the equatorward boundary of the plasma sheet. Recent measure-
ments of electric fields near the "inverted V" electron precipitation bands
suggests that these events are associated with large electrostatic potential
gradients along the geomagnetic field.

Introduction

    The importance of electric field measurements for studying the convective motions
of plasma in the magnetosphere has been recognized for a number of years [Dungey, 1961;
Axford and Hines, 1961; Piddington, 1962; Axford, 1969]. Only recently, however, have
adequate techniques been developed to provide a comprehensive survey of electric fields
in the magnetosphere. Electric field measurements with satellites [Cauffman and Gurnett,
1971; Heppner, 1972a] and ionized Barium cloud releases [Haerendel and Lust, 1970;
Wescott et al., 1969] have now established the primary features of magnetospheric plas-
ma convection at low altitudes over the auroral zones and polar caps. Since electric
fields must ultimately be responsible for the acceleration and energization of charged
particles in the magnetosphere, it is of great interest to determine the relationships
between the electric fields and plasmas in the magnetosphere. Although extensive meas-
urements of low-energy charged particles have been obtained [see the review by Hultquist,
1969, and the spatial survey by Frank and Ackerson, 1972] until recently the relation-
ship between electric fields and charged particle intensities has been largely unex-
plored. In this paper we review the primary features of the electric field distribution
over the auroral zones and polar caps as revealed by low-altitude polar orbiting sate-
llites and discuss the relationship of these electric fields to the various plasma re-
giems of the magnetosphere as revealed by our current investigations.

Survey of Auroral Zone and Polar Cap Electric Fields

    Although numerous techniques, including Barium cloud releases and balloon-borne
electric field measurements [Mozer and Serlin, 1969], have been employed in the meas-
urement of auroral zone and polar cap electric fields, it is the recent advent of
satellite measurements using the double-probe technique which has produced a compre-
hensive picture of these high-latitude electric fields. The first global survey of
convection electric fields was obtained from the double-probe electric field experiment
on the low-altitude (677 to 2528 km) polar orbiting satellite Injun 5 launched in
August, 1968. Figure 1 from Cauffman and Gurnett [1971] shows a series of dawn-dusk

passes over the northern polar region selected to illustrate the primary features of the high-latitude convection electric fields observed by Injun 5. The arrows in Figure 1 give the direction and magnitude of the convection velocity component measured, as computed from

$$\vec{V}_c = \frac{\vec{E}_c \times \vec{B}}{B^2} \quad ,$$

where $\vec{E}_c$ is the measured electric field (after subtracting the $\vec{V} \times \vec{B}$ field due to the spacecraft motion through the ionosphere) and $\vec{B}$ is the local geomagnetic field vector. Since only one component of the electric field was measured by Injun 5, only the components of the convection velocity indicated by the arrows could be determined on any single pass.

The most prominent and persistent feature of the Injun 5 electric field data is the occurrence of an abrupt reversal in the convection velocity and electric field at about 70° to 80° invariant latitude. These reversals are particularly evident in Figure 1 at about 1724:20, 1925:30 and 2123:30 UT in the dawn local time region and at 1734:00 and 2132:00 UT in the dusk local time region. In all cases, the reversals are consistent with a generally sunward flow on the equatorward side of the reversal and an anti-sunward flow on the poleward side of the reversal. The largest convection velocities are usually found within about 5° to 10° invariant latitude of the electric field reversal location. The convection velocities often exhibit a pronounced dawn-dusk asymmetry (evident in orbits 6910 and 6911 of Figure 1) with small, or near zero, convection velocities over a significant portion of the polar cap region. However, in some cases (such as orbit 6909 of Figure 1) the anti-sunward flow is nearly uniform along the entire satellite trajectory over the polar cap region. Only about 14% of the Injun 5 polar passes can be characterized as having uniform anti-sunward flow over the polar-cap region comparable to orbit 6909.

The OGO-6 satellite, launched in June 1969 into a low-altitude near polar orbit, also carried a double-probe electric field experiment [Heppner, 1972a] which shows many of the same features of the high-latitude convection revealed by Injun 5. The electric field for a series of dawn-dusk passes of OGO-6 over the northern hemisphere is shown in Figure 2 [these data were kindly provided by J. Heppner and T. Aggson]. The electric antenna axis during this series of passes is oriented approximately perpendicular to the spacecraft-sun line so the electric field directly indicates the sunward (positive) and anti-sunward (negative) component of the plasma convection velocity. Electric field reversals are evident in both the dawn and dusk regions, separating the region of generally anti-sunward flow over the polar cap from the sunward flow at lower latitudes. These data clearly illustrate the large variability in the anti-sunward plasma flow over the polar region, ranging from nearly uniform flow (as in orbits 64, 83, and 121) to very asymmetrical flow patterns with large convection velocities near one of the reversals and near zero convection velocities on the opposite side of the polar region (as in orbits 130, 155, 184, 208, 222, 226, and 236).

Figures 1 and 2 illustrate the close similarity between the Injun 5 and OGO-6 convection electric field observations in the dawn-dusk meridional plane. Qualitatively both sets of data show (1) the persistent occurrence of electric field reversals at about 70° to 80° invariant latitude, (2) the occurrence of generally anti-sunward convection poleward of the electric field reversal and sunward convection equatorward of the electric field reversal, (3) the large variability in the profile of the anti-sunward plasma flow over the polar region, ranging from nearly uniform profiles in some cases to very asymmetrical profiles, with large differences between the dawn and dusk, in other cases. The only quantitative disagreement between these two sets of data appears to be in the relative occurrence and emphasis of the different types of anti-sunward convection profiles. Whereas the Injun 5 data show that cases of relatively uniform anti-sunward convection over the polar region, such as orbit 6909 in Figure 1, are relatively uncommon ($\sim$ 14%) the examples shown by Heppner [1972a] give the impression that nearly uniform anti-sunward flow is the most common form of plasma flow over the polar region. Heppner [1972b] has recently emphasized that asymmetric convection

profiles are also frequently observed in the OGO-6 data, as evident from Figure 2, and has established a relationship of these convection profiles with the direction of the interplanetary magnetic field.

The general features of the high-latitude electric fields at other local times have been obtained by Cauffman and Gurnett [1972] from a survey of all of the Injun 5 electric field data. The electric field reversals evident in the dawn-dusk passes of Figures 1 and 2 are a consistent feature of the high-latitude electric field data at all local times except in the local evening and local midnight regions. In these regions electric field reversals are also observed, however the electric field variations are usually more complex and variable, often consisting of multiple reversals and large fluctuations which cannot be simply identified as a single electric field reversal. The main features of the high-latitude convection pattern deduced from these data are summarized in Figure 3. The two diagrams of Figure 3 are intended to emphasize the variability of the convection pattern, from distinctly non-uniform anti-sunward flow over the polar cap region, as in (a), to nearly uniform anti-sunward flow over the polar cap region, as in (b). The dashed line in Figure 3, separating the regions of sunward and anti-sunward flow, is the average location of the electric field reversal obtained from the Injun 5 data by Cauffman and Gurnett [1972]. It must be emphasized that these convection diagrams represent a gross average and the actual convection pattern may differ markedly from these "average" patterns. Major departures include:

(1) dawn-dusk asymmetries in the convection, usually consisting of marked differences in the size and intensity of the dawn and dusk convection cells,

(2) multiple reversals and irregular fluctuations, particularly in the local evening, possibly indicative of a turbulent eddy-like convection pattern in these regions,

(3) variations in the location of the "stagnation point" for the east-west plasma flow near local noon, and

(4) temporal variations in the latitude of the electric field reversal.

The anti-sunward convection over the polar region and the associated two-cell convection pattern inferred from these measurements provide strong evidence of the merging of the geomagnetic field lines with the interplanetary magnetic field as suggested by Dungey [1961]. Frank and Gurnett [1972] have shown that the electric field reversal corresponds to the boundary between "open" magnetic field lines, which connect into the solar wind, on the poleward side of the reversal and "closed" field lines, which connect to the opposite hemisphere without crossing the magnetopause, on the equatorward side of the reversal. An observational model which accounts for the nonuniform anti-sunward convection of magnetic field lines over the polar regions has been presented by Frank [1971a, b] and Frank and Gurnett [1971].

Electric Field Reversals and the Electron $E > 45$ keV Trapping Boundary

In an initial investigation of electric fields and their association with charged particle intensities Frank and Gurnett [1971] found that the "trapping boundary" for electrons with energies $E > 45$ keV is located essentially coincident with the electric field reversal. This relationship is illustrated in Figure 4, which shows the electric field and charged particle intensities for a dawn-dusk pass over the northern polar region. The electron $E > 45$ keV trapping boundary, which is observationally identified with the high-latitude termination of measurable $E > 45$ keV electron intensities, is shown by the vertical dashed lines at 1443 and 1453 UT. The electric field measurements obtained during this pass display a clearly defined electric field reversal, separating regions of sunward and anti-sunward convection, at about 1443 UT in the local dawn region and a less distinct reversal at 1453 UT in the local dusk region. The electric field reversal in the local dawn is seen to be located essentially coincident with the electron $E > 45$ keV trapping boundary. Examination of numerous other passes at various

local times has shown that when an electric field reversal can be clearly identified, the electron $E > 45$ keV trapping boundary is almost always located essentially coincident with the electric field reversal. Since open magnetic field lines cannot sustain trapped energetic electron intensities, the observed correspondence between the electron $E > 45$ keV trapping boundary and the electric field reversal provides further evidence that the electric field reversal corresponds with the boundary between open and closed magnetic field lines.

An unusual case in which the trapping boundary does not correspond with the location of the electric field reversal is shown in Figure 5. This pass occurred just preceding the expansion phase of a substorm [Gurnett and Frank, 1973]. In the local evening region of this pass the electron $E > 45$ keV trapping boundary is located at about 1516:00 UT, several degrees equatorward of the electric field reversal at 1519:00 UT and in the zone of sunward convection. In this case we attribute the poleward movement of the electric field reversal, relative to its usual position near the trapping boundary, as being due to the rapid reconnection and creation of "new" closed field lines in the distant plasma sheet which are not yet populated by energetic ($E > 45$ keV) electrons. The region of sunward plasma flow in the local evening sector is also associated with the enhanced low-energy electron and proton intensities shown by the shaded band in Figure 12. From the relatively soft energy spectrums and overall intensities of these particles and their location on closed magnetic field lines, this region of low-energy electron and proton intensities has been identified with the plasma sheet along the evening flanks of the magnetosphere [Gurnett and Frank, 1972b]. This identification of plasma-sheet electrons and protons poleward of the trapping boundary and in the region of sunward convection (the shaded part of Figure 5) provides substantial evidence of the increased reconnection rate and creation of new closed field lines in the plasma sheet during the initial phase of the substorm. One hour later, during the decay phase of the substorm, the electric field reversal is observed to have relaxed back to its usual position near the electron $E > 45$ keV trapping boundary.

Electric Fields and Auroral Particle Precipitation

From the observations of Frank [1971a], it is known that plasma from the dayside magnetosheath has direct access into the high-latitude magnetosphere through a region called the polar cusp. Figure 6 illustrates a meridional pass by Injun 5 [Gurnett and Frank, 1972b] through the polar cusp region in the early-afternoon local time sector. The polar cusp region, encountered on this pass from about 0850:10 to 0852:10 UT, is easily identified by the enhanced intensities of low-energy electrons ($105 \leq E \leq 185$ eV) and protons ($290 \leq E \leq 455$ eV) shown shaded in Figure 6. The polar cusp region is located adjacent to and poleward of the electron $E > 45$ keV trapping boundary indicated by the vertical dashed line at about 0850:10 UT. The enhanced low-energy electron intensities occur in a narrow latitudinal band located essentially coincident with the electron $E > 45$ keV trapping boundary. The polar cusp proton fluxes occur in a somewhat broader zone extending several degrees invariant latitude poleward of the trapping boundary. The intense broad-band VLF hiss shown in the top panel of Figure 6 is believed to be generated by the low-energy (~ 100 eV) polar cusp electrons [Gurnett and Frank, 1972a]. The electric field measurements for this pass, in the second panel from the top in Figure 6, show a clearly defined electric field reversal at about 0850:10 UT, coincident with the electron $E > 45$ keV trapping boundary and at the equatorward boundary of the polar cusp region. A polar diagram showing the convection velocity components associated with these electric field measurements is shown in Figure 7. The plasma convection in the polar cusp region is eastward and in a generally anti-sunward direction indicating that the polar cusp plasma is on "open" field lines which connect with the solar wind magnetic field through the dayside magnetosheath. The westward plasma flow equatorward of the electric field reversal, within the region of measurable electron $E > 45$ keV intensities, constitutes the return flow of plasma on closed field lines toward the dayside magnetopause.

Frank and Ackerson [1972] have shown that when the low-energy electron precipitation band in the polar cusp is followed around into the local evening, the average energy of the precipitation bands have a characteristic "inverted V" energy-time signa-

ture in which the average electron energy increases to a maximum and subsequently decreases as the spacecraft passes through the precipitation region [Frank and Ackerson, 1971]. These "inverted V" electron precipitation bands have been directly associated with visible auroral arcs [Ackerson and Frank, 1972].

The precipitated electron energy flux associated with a series of "inverted V" events observed in the early local evening sector is shown in Figure 8. The most intense "inverted V" event on this pass was encountered from about 0027:45 to 0028:05 UT, as indicated by the large increase in the electron energy flux during this interval, up to $\sim$ 10 ergs $(cm^2\text{-sec-sr})^{-1}$. Color energy-time spectrograms which clearly show the "inverted V" characteristic of this event are being published separately [Gurnett and Frank, 1972b]. As is typical of these events [Frank and Ackerson, 1971], the "inverted V" electron precipitation band is located poleward of the electron $E > 45$ keV trapping boundary.

Frank and Gurnett [1971] have shown that "inverted V" electron precipitation events are closely associated with electric field reversals. This relationship is evident from the electric field data in Figure 8 which shows a highly structured discontinuity in the electric field, indicative of an electric field reversal, from about 0027:45 to 0028:05 UT. The location of this electric field reversal is seen to be essentially coincident with the location of the "inverted V" event observed on this pass. Other similar data showing the occurrence of "inverted V" events coincident with the electric field reversal have been presented by Frank and Gurnett [1971].

In the late evening and midnight local time regions, where electric field reversals are often not clearly distinguishable, the "inverted V" electron precipitation events still have a distinctive signature in the electric field data. An example of an "inverted V" event on a pass through the local midnight region is shown in Figure 9. A very distinct "inverted V" event with a maximum electron energy flux of about 20 ergs $(cm^2\text{-sec-sr})^{-1}$ occurred from about 0622:55 to 0623:25 UT and several less distinct "inverted V" events of lower energy flux occurred from 0623:25 to 0624:45 UT. The electron energy-time spectrogram for this pass is shown in Figure 7 of Frank's [1972] paper for this symposium.

As can be seen from the top panel of Figure 9 the electric field in the neighborhood of the "inverted V" events is characterized by large, $\sim$ 50 mV $(m)^{-1}$ irregular fluctuations on a time scale of a few seconds. The most striking feature of these electric field variations is the $\sim$ 125 mV $(m)^{-1}$ south-eastward spike in the electric field at 0622:55 UT and the similar, but oppositely directed (north-westward) spike at 0623:50 UT. As indicated by the vertical guide lines in Figure 9, these spikes correspond very closely with the boundaries of the most intense "inverted V" event observed during this pass. Note that the energy flux of the "inverted V" event is not located symmetrically relative to the spatial configuration of these oppositely directed fields. Irregular fluctuation in the electric field, often consisting of distinct pairs of oppositely directed spikes as in Figure 9, are a persistent feature of all "inverted V" events observed with Injun 5. In many cases these irregular fluctuations provide such a distinctive "signature" that the location of the "inverted V" events could be determined with good reliability from the electric field measurement alone without prior reference to the plasma observations.

The broad region of somewhat lower electron energy flux from about 0624:45 to 0627:30 UT in Figure 9 has been identified as the plasma sheet by Gurnett and Frank [1972b] from electron energy spectrums and intensities characteristic of this region. Within the plasma sheet region the large irregular electric field fluctuations associated with the "inverted V" event have disappeared and the electric field variations are relatively smooth. Near the equatorward boundary of the plasma sheet the electric field increases to about 65 mV $(m)^{-1}$ and abruptly decreases to near zero at the equatorward boundary of the plasma sheet, which also corresponds closely with the plasmapause location on this pass. Similar large convection electric fields have been observed deep within the magnetosphere on other passes in the local midnight region [Gurnett and Frank, 1972b] indicating that electric fields may be more important than previously

thought for the transport, loss, and de-energization of plasma sheet particles penetrating into this region of the magnetosphere [see discussions by Vasylinunas, 1968; and Kennel, 1969].

Electric Fields and Visual Aurora

Since electric field measurements are readily obtained from Barium cloud releases under conditions when auroral light emissions can be observed [Wescott et al., 1969; Haerendel and Lust, 1970], it is important to relate the charged particle/electric field measurements obtained via satellites to ground observations of visual aurora. Because of the difficulty in obtaining suitable simultaneous satellite and ground data, no direct comparison of satellite electric field measurements with auroral light emissions have yet been reported.

In attempting to relate auroral light emissions to the electric field and plasma observations obtained by Injun 5, it is important to recognize the distinction, made by Frank and Ackerson [1971, 1972], between the "inverted V" electron precipitation bands and the adjacent but equatorward precipitation from the plasma sheet. During magnetically quiescent periods the precipitated energy flux in the local evening is usually dominated by the "inverted V" bands (see Figures 8 and 9, for example). Ackerson and Frank [1972] clearly show that the "inverted V" bands produce visible auroral arcs. Although the precipitated energy flux from the "inverted V" bands is usually greater, the plasma sheet electron precipitation is also sufficiently intense to produce auroral light emission equatorward of the "inverted V" precipitation. During the expansion phase of a substorm the precipitated energy flux from the plasma sheet increases considerably [Ackerson, 1972] and for these periods the dominant auroral light emission is probably from the plasma sheet region. Since the "inverted V" electron precipitation band is usually located near or slightly poleward of the electric field reversal and the plasma sheet precipitation occurs equatorward of the electric field reversal, it is clearly important to distinguish these two precipitation regions when analyzing associations with auroral light observations. At this time, it is not clear how, or whether, these precipitation regions can be identified from visual auroral observations alone.

Evidence of Parallel Electric Fields

For several years [Alfven, 1958; Carlqvist and Bostrom, 1970] it has been believed that electric fields parallel to the geomagnetic field may be responsible for auroral charged particle acceleration. Although direct measurements of parallel electric fields have been reported [Mozer and Fahleson, 1970] the existence of these fields and their relationship to the auroral charged particle acceleration has been quite uncertain and speculative. The identification of "inverted V" electron energy-time spectra and the discovery of oppositely directed, spike-like electric fields at the boundaries of the "inverted V" events, as in Figure 9, provides us with convincing new evidence that parallel electric fields are responsible for the electron acceleration in these events. As commented by Frank and Gurnett [1971] the unique energy spectrum of the "inverted V" events and their anisotropic distribution of electron intensities downward along the magnetic field is in itself strongly suggestive of acceleration by an electrostatic potential gradient along the geomagnetic field. The "inverted V" energy-time variation is easily accounted for by a potential difference along the magnetic field which varies from near zero at the boundaries of the "inverted V" to a maximum at the peak of the "inverted V". Qualitatively, the resulting electrostatic potential contours within the "inverted V" region must be as shown in Figure 10. The electrons in the "inverted V" events are believed to originate from the magnetosheath [Frank and Ackerson, 1971] with energies on the order of 100 eV. The spread in electron energies commonly observed for the "inverted V" events, indicated by the crosshatching in Figure 10, is thought to be due to heating or scattering from plasma instabilities in the precipitated electron beam, and is possibly related to the intense VLF hiss emissions associated with these events [Gurnett and Frank, 1972a].

The oppositely-directed spikes in the electric field at the boundaries of the "inverted V", as in Figure 9, are readily explained by the electric fields which develop

near the boundaries of the "inverted V" as shown in Figure 10. If the electric field is zero outside of the "inverted V" the potential from the spacecraft to the base of the acceleration region, Φ_s, can be obtained by integrating the $\vec{E}_\perp$ electric field component along the satellite trajectory. A rough estimate of this integral for the case shown in Figure 9 gives a maximum value for Φ_s of ~ 6 kV. Since the maximum electron energy of the "inverted V" is about 15 keV, it is evident that a significant portion of the electron acceleration must take place below the satellite, which was at an altitude of about 2400 km in this case. Because the "inverted V" electron precipitation events involve a significant current parallel to the geomagnetic field [Frank and Ackerson, 1971] it seems most likely that this field-aligned "Birkeland" current is an important factor is producing these potential gradients along the geomagnetic field. Whether the mechanism responsible for these field-aligned potential gradients is a space-charge region of the type discussed by Carlqvist and Bostrom [1970] or an anomalous resistivity produced by a plasma instability, as discussed by Kindel and Kennel [1971], remains to be determined.

Acknowledgments

References

Ackerson, K. L. Observations of charged particle precipitation over the auroral zone during a magnetic substorm, Submitted for publication, J. Geophys. Res., 1972.

Ackerson, K. L., and L. A. Frank, Correlated satellite measurements of low-energy electron precipitation and ground-based observations of a visible auroral arc, J. Geophys. Res., 77, 1128, 1972.

Alfven, H., On the theory of magnetic storms and aurorae, Tellus, 10, 104, 1958.

Axford, W. I., Magnetospheric convection, Reviews of Geophys., 7, 421, 1969.

Axford, W. I., and C. O. Hines, A unifying theory of high-latitude geophysical phenomena and geomagnetic storms, Can. J. Phys., 39, 1433, 1961.

Carlqvist, P., and R. Bostrom, Space charge regions above the aurorae, J. Geophys. Res., 75, 7140, 1970.

Cauffman, D. P., and D. A. Gurnett, Double-probe measurements of convection electric fields with the Injun 5 satellite, J. Geophys. Res., 76, 6014, 1971.

Cauffman, D. P., and D. A. Gurnett, Satellite measurements of high-latitude convection electric fields, Accepted for publication, Space Sci. Rev., 11, 1972.

Dungey, J. W., Interplanetary magnetic field and auroral zones, Phys. Rev. Lett., 6, 47, 1961.

Frank, L. A., Plasma in the earth's polar magnetosphere, J. Geophys. Res., 76, 5202, 1971a.

Frank, L. A., Comments on a proposed magnetospheric model, J. Geophys. Res., 76, 2512, 1971b.

Frank, L. A., Plasma entry into the earth's magnetosphere, Paper B.2.1 of the 1972 COSPAR Symposium on Critical Problems of Magnetosphere Physics, Madrid, Spain, 1972.

Frank, L. A., and K. L. Ackerson, Observations of charged particle precipitation into the auroral zone, J. Geophys. Res., 76, 3612, 1971.

Frank, L. A., and K. L. Ackerson, Local-time survey of plasma at low altitudes over the auroral zones, in press, J. Geophys. Res., 1972.

Frank, L. A., and D. A. Gurnett, Distributions of plasmas and electric fields over the auroral zones and polar caps, J. Geophys. Res., 76, 6829, 1971.

Gurnett, D. A., and L. A. Frank, VLF hiss and related plasma observations in the polar magnetosphere, J. Geophys. Res., 77, 172, 1972a.

Gurnett, D. A., and L. A. Frank, Observed relationships between electric fields and auroral particle precipitation, submitted for publication, J. Geophys. Res., 1972b.

Haerendel, G., and R. Lust, Electric fields in the ionosphere and magnetosphere, Particles and Fields in the Magnetosphere, B. M. McCormac, ed., Reinhold Book Company (Dordrecht, Holland), 213, 1970.

Heppner, J. P., Electric field variations during substorms: OGO-6 measurements, Rep. X-645-72-10, Goddard Space Flight Center, Greenbelt, Md., 1972a.

Heppner, J. P., High-latitude electric fields, Trans. Am. Geophys. Union, 53(4), (title only), 360, 1972b.

Hultqvist, B., Auroras and polar substorms: Observations and theory, Rev. Geophys., 7, 129, 1969.

Kennel, C. F., Consequences of a magnetospheric plasma, Rev. Geophys., 7, 379, 1969.

Mozer, F. S., and U. V. Fahleson, Parallel and perpendicular electric fields in an aurora, Planet. Space Sci., 18, 1563, 1970.

Piddington, J. H., A hydromagnetic theory of geomagnetic storms and auroras, Planet. Space Sci., 9, 947, 1962.

Vasylinunas, V. M., A survey of low-energy electrons in the evening sector of the magnetosphere with OGO 1 and OGO 3, J. Geophys. Res., 73, 2839, 1968.

Wescott, E. M., J. D. Stolarik, and J. P. Heppner, Electric fields in the vicinity of auroral forms from motions of barium vapor releases, J. Geophys. Res., 74, 3469, 1969.

Figure Captions

Figure 1.   The convection velocity components determined for a series of dawn-dusk orbits of Injun 5 over the northern hemisphere. Note the persistent occurrence of electric field reversals at about 70° to 80° invariant latitude separating the anti-sunward plasma flow poleward of the reversal from the sunward flow at lower latitudes.

Figure 2.   The dawn-dusk electric field observed for a sequence of dawn-dusk orbits of OGO-6 over the northern hemisphere. Note the occurrence of both uniform and asymmetrical anti-sunward convection profiles over the polar region.

Figure 3.   Schematic diagram showing "average" convection patterns observed by Injun 5 and OGO-6, ranging from (a) distinctly non-uniform and often asymmetrical anti-sunward flow over the polar region to (b) essentially uniform anti-sunward flow over the entire polar cap.

Figure 4.   Simultaneous electric field and charged particle measurements showing the correspondence between the electric field reversals at 1443 and 1453 UT and the electron $E > 45$ keV trapping boundary (vertical dashed lines).

Figure 5.   An unusual case during the initial phase of a substorm in which the electric field reversal at 1519 UT is located several degrees poleward of the electron $E > 45$ keV trapping boundary at 1516 UT.

Figure 6.   Simultaneous observations of VLF hiss, convection electric fields, and charged particle intensities for a noon-midnight meridional pass over the southern polar cap and auroral zone. Note that the polar cusp is located in the zone of eastward convection just poleward of the electric field reversal and the electron ($E > 45$ keV) trapping boundary (see Figure 7).

Figure 7.   A polar diagram showing the direction and magnitude of the convection velocity components associated with the electric field observations in Figure 6.

Figure 8.   An early-evening pass showing a series of "inverted V" electron precipitation events located coincident with the electric field reversal at about 0027:45 to 0028:05 UT.

Figure 9.   A pass near local midnight showing oppositely directed "spikes" in the electric field at the boundaries of the "inverted V" event from 0622:55 to 0623:50 UT and a large zone of plasma convection near the equatorward boundary of the plasma sheet.

Figure 10. Qualitative form of the electrostatic potential contours associated with an "inverted V" electron precipitation event. Note the oppositely directed $E_\perp$ electric field at the boundaries of the "inverted V", similar to the case shown in Figure 9.
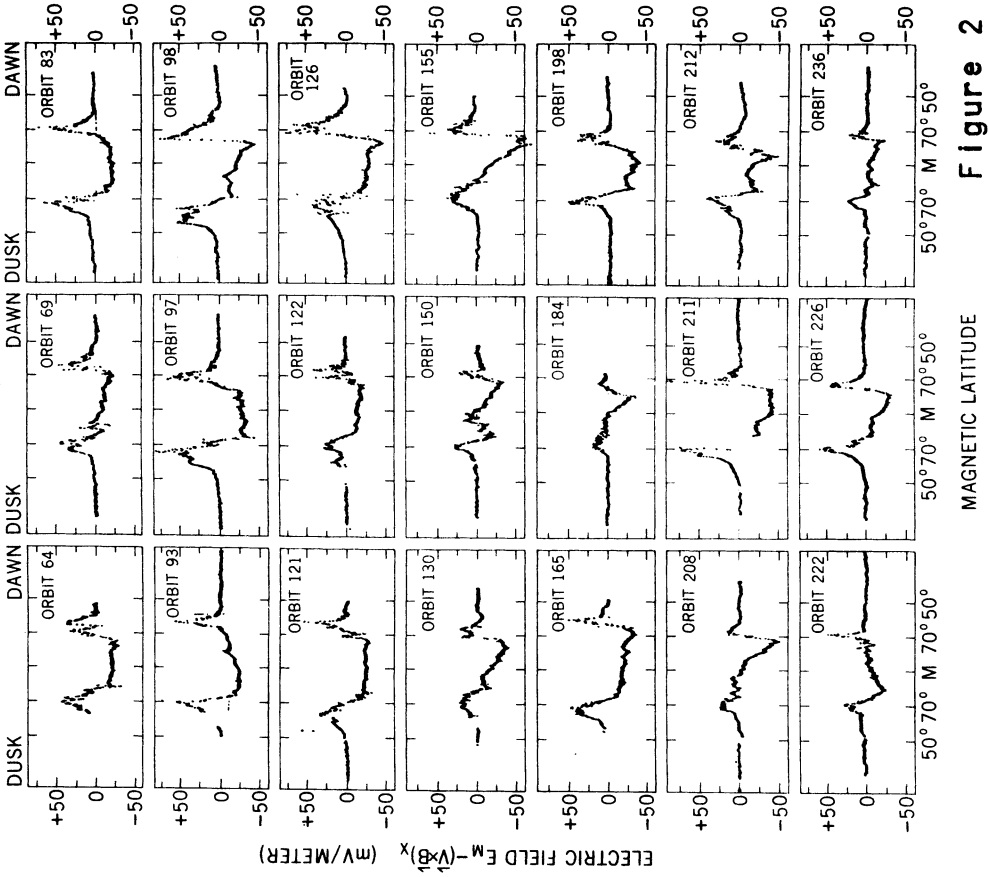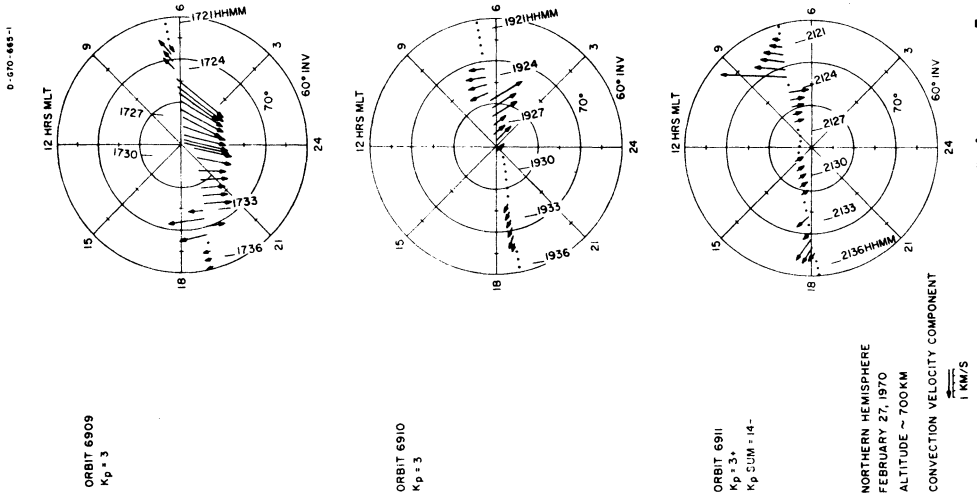
OGO-6 N HEMISPHERE PASSES
JUNE 10-22, 1969

Figure 2

MAGNETIC LATITUDE

ELECTRIC FIELD E_m $-(V \times B)_x$ (mV/METER)

Figure 1

ORBIT 6909
$K_p = 3$

ORBIT 6910
$K_p = 3$

ORBIT 6911
$K_p = 3+$
K_p SUM = 14−

NORTHERN HEMISPHERE
FEBRUARY 27, 1970
ALTITUDE ~ 700 KM
CONVECTION VELOCITY COMPONENT
1 KM/S

D-GTO-665-1

132

Figure 4

(a) MAXIMUM CONVECTION VELOCITIES NEAR THE ELECTRIC FIELD REVERSAL BOUNDARY

(b) NEARLY UNIFORM CONVECTION OVER THE POLAR CAP

SUNWARD CONVECTION (> .75 KM/SEC)
ANTI-SUNWARD CONVECTION (> .75 KM/SEC)
CONVECTION VELOCITY (< .75 KM/SEC)
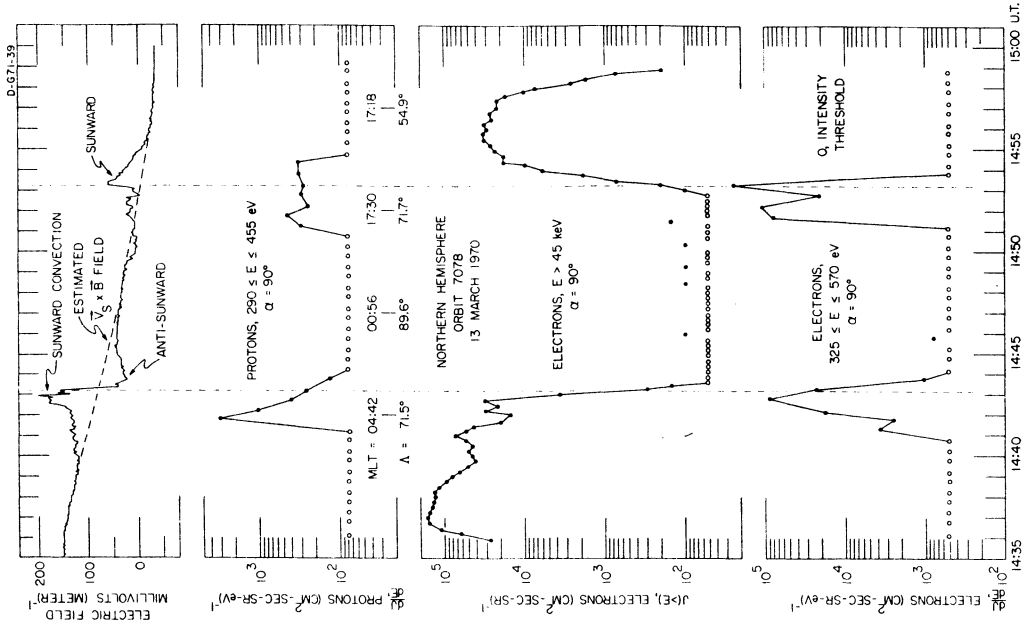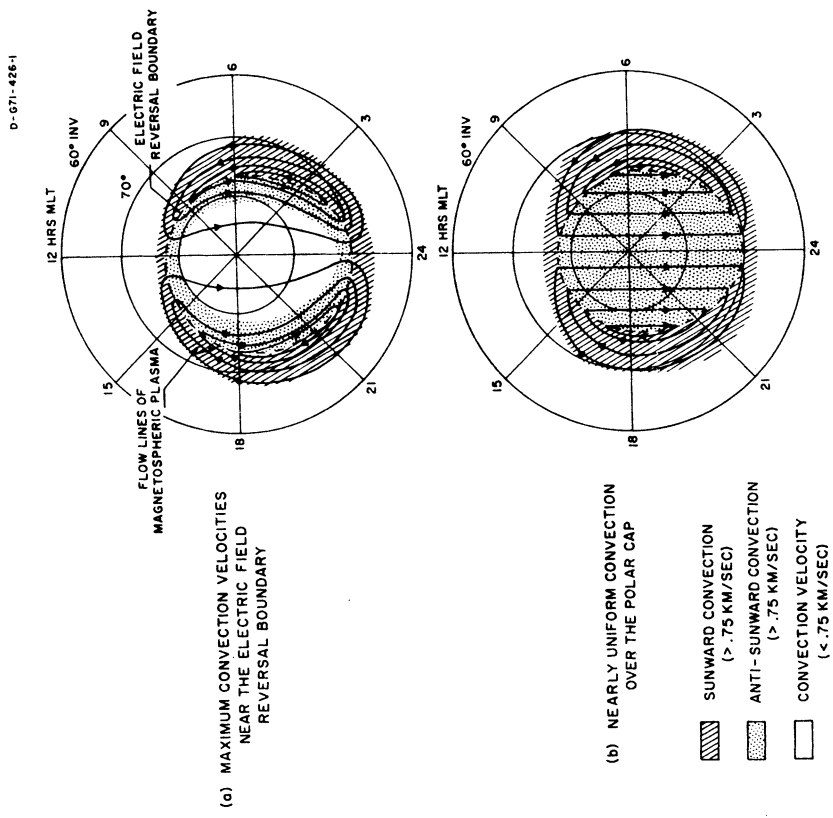
Figure 3
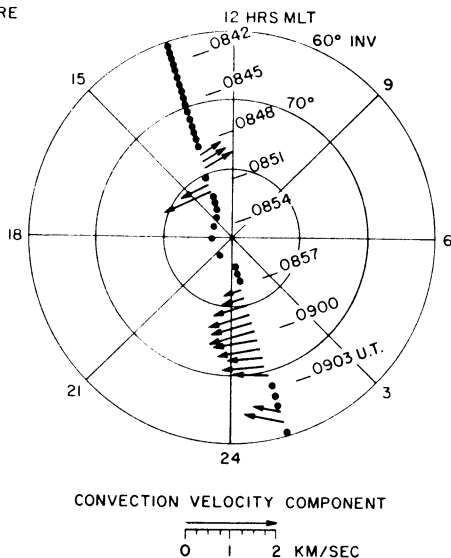
Figure 6

Figure 5
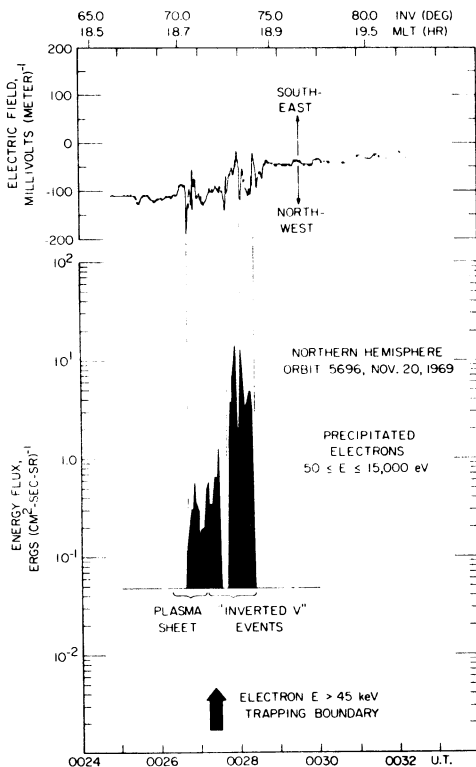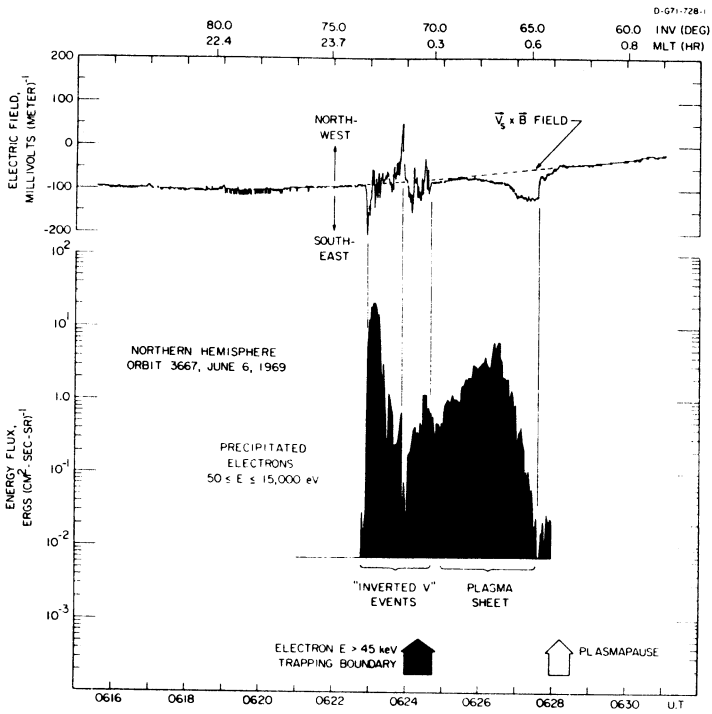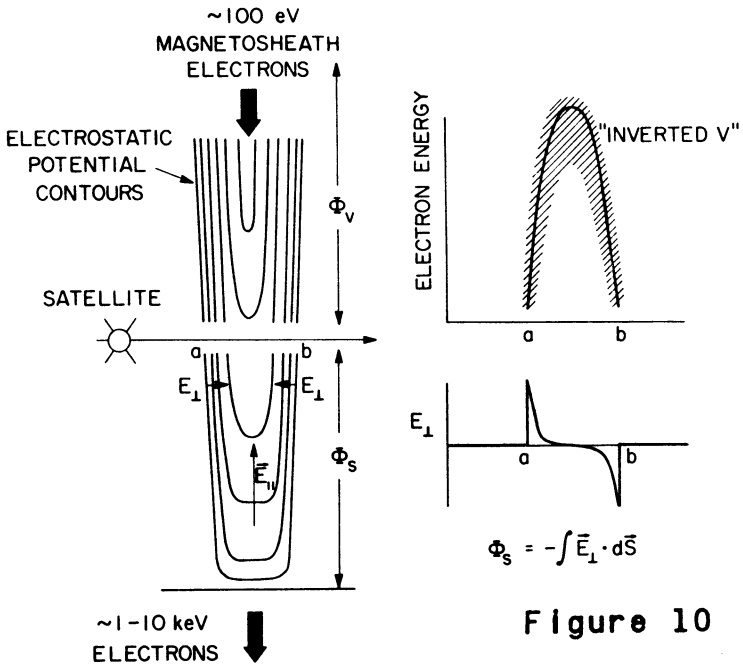
Figure 7

Figure 8

Figure 9

Figure 10

136

Riedler: Did you measure pitch-angle distributions? If so, how do they fit the double-layer picture (parallel electric fields) in the 'inverted V' regions?

Gurnett: Yes, we measured the electron intensities parallel and perpendicular to the local magnetic field vector. Qualitatively, the angular distribution of electron intensities agrees with the idea that an electric field parallel to the geomagnetic field must occur in the 'inverted V' region, since the downgoing flux parallel to the geomagnetic field exceeds the flux perpendicular to the geomagnetic field by a large factor. To reach a definitive conclusion about the existence of double-layers, however, will require better resolution of the pitch-angle distribution than is available with Injun 5. Such measurements are now being made by Dr. Frank with a LEPEDEA experiment on the UK-4 satellite.

Heikkila: First I would like to make three comments: (1) Electrons with energies $325 < E < 570$ eV are not a good indicator of the cusp, since the peak in the spectrum often occurs below 100 eV, even as low as 30 eV. (2) The trapping boundary is not synonymous with the outer boundary of the plasma sheet; the Vela data show that the distant plasma sheet is generally populated by much cooler plasma. I cannot agree that the 'inverted V' events are always on open field lines. (3) The polar caps are by no means devoid of soft particles; such fluxes can at times be large.

My question is, do the northern and southern stagnation points in the E-field reversal occur at the same local times?

Gurnett: First, let me comment on your comments. (1) we normally use the low-energy (100 to 500 eV) proton intensities to identify the polar cusp locations, provided the proton intensities are above our background rate. The $105 \leq E \leq 185$ eV electron intensities shown in Figure 6 are intended to illustrate the occurrence of intense fluxes of $\sim$ 100 eV electrons in the polar cusp which are associated with the VLF hiss emissions. (2) I did not mean to give the impression that we only use the electron $E > 45$ keV trapping boundary to identify the plasma sheet. The plasma sheet is identified by comparing the energy spectrum and absolute intensities of both electrons and protons with measurements by essentially identical LEPEDEA instrumentation which have been obtained by Dr. Frank through the plasma sheet at high altitudes near the equatorial plane. Since the 'inverted V' events are usually observed at the location of the electric field reversal, it is clear that these events occur very close to the boundary between open and closed field lines. By measuring the bounce period of $E > 45$ keV electron packets in the plasma sheet, Frank and Ackerson have shown that the lengths of the field lines in the 'inverted V' region are very long -- greater than 50 R_E. Since 'inverted V' events have been observed poleward of the electric field reversal, it is our opinion that these events are located on open field lines and that the electron flux in the 'inverted V' originates from the magnetosheath. (3) We agree: the polar caps do at times have large fluxes.

In answer to your question, we have not investigated the possibility of an asymmetry in the location of the northern and southern hemisphere stagnation points.

DeForest: Have simultaneous phase-space spectra been made of magnetosheath plasma and 'inverted V' plasma? This could be an easy check to see if magnetosheath is the source of 'inverted V's'.

Frank: No, we have not yet made a simultaneous comparison of the phase-space density of the magnetosheath plasma and the 'inverted V' plasma.

Fälthammar: From the last two presentations it appears that the electric field over the polar cap, after subtraction of the $V \times B$ field, is often zero (within the accuracy of measurement) according to Injun 5 measurements, but generally distinctly nonvanishing according to OGO-6 measurements. Is there a systematic difference of this kind, or is it only a matter of different instrumental thresholds?

Gurnett: Frequently in the Injun 5 data the electric field is near zero, less than $10 \text{ mV} \text{ m}^{-1}$, over a sizable portion of the polar cap region. Figures 4 and 6 show examples of such cases. Our accuracy in many of these cases is very good and there can be no doubt that in many cases there is a sizable region poleward of the electric field reversal within which the convection electric field is much smaller than it is near one or both of the electric field reversals. The OGO-6 data in Figure 2 clearly shows examples where the electric field is small over a portion of the polar cap (see orbits 69, 130, 150, 155, 184, 208, 222, and 236) so I think that this feature is characteristic of both sets of data. Since the OGO-6 antenna is about 10 times longer than the Injun 5 antenna, the OGO-6 experiment is more sensitive than the Injun 5 experiment. However, we have many cases with Injun 5 in which the antenna orientation and rotation

Proceedings of the Symposium jointly sponsored by

COSPAR, IAGA, and URSI; Madrid, Spain, 11-13 May 1972.